Numerical Study of Ship Rolling in Turning Manoeuvres

Serge Sutulo, *Unit of Marine Technology and Engineering, Technical University of Lisbon*

Instituto Superior Técnico

C. Guedes Soares, *Unit of Marine Technology and Engineering, Technical University of Lisbon*

Instituto Superior Técnico

ABSTRACT

A unified mathematical model describing both manoeuvring and seakeeping motions of surface displacement ships is used for numerical investigation of the ship motions in turning manoeuvres under action of regular waves. The 6DOF model combines a semi-empiric model for the still-water manoeuvring forces with a model for the seakeeping forces built as a generalization of the ordinary strip method. Comparative simulations included unrestrained and restrained straight runs in beam seas, and turning manoeuvres in still water and under action of waves, and are demonstrating that the attained instantaneous roll angles can be higher in turning than in the straight run.

Keywords: turning manoeuvre, rolling, regular waves, simulation.

1. INTRODUCTION

Historically, the ship rolling was the first kind of ship motions in waves studied theoretically and it remained the most important one from the viewpoint of the ship safety. While the first studies were dealing with a ship at zero speed and subject to the action of regular beam seas, further developments of the theory accounted for the speed of advance and already at arbitrary wave encounter angles.

Instead of simpler mathematical models based on an isolated roll equation, effects of coupling were accounted for leading to sophisticated 6DOF time-domain simulation codes. Also, consideration of the irregular waves, and/or nonlinear phenomena, such as the parametric and sub-harmonic resonance etc. was done.

At the same time, one basic assumption, which can be considered as traditional for the seakeeping in general, was kept unchanged: the reference motion of the ship was assumed to be a rectilinear motion with constant speed and zero mean drift angle. In fact, the problem statement involving this assumption not only is the simplest possible but is also reasonable and rather well based. First of all, running in straight path is the predominant regime for most seagoing vessels. Another typical situation is stationing, i.e. free drifting or positioning, at zero speed but this is just a particular case of the previous situation. Any sort of manoeuvring takes only a small fraction of many ships' operational time.

Also, from certain viewpoints, the straight run can occur to be one of the most dangerous options: in the case of an unfavourable combination of the parameters of the incident waves and of the ship's speed and heading, any possible resonance will benefit from a long and steady exposure and will be able to develop up to a possible critical situation.

On the other hand, however, it is known from the maritime practice that manoeuvres in stormy weather can become dangerous and are to be avoided completely or should be performed in a gentle and careful way as otherwise the combined effect of the manoeuvre-induced roll

and of the wave action can result in fatal consequences. But there are many situations when hard manoeuvring in extremely rough sea cannot be avoided: rescue and salvage operations, weapon- or collision-avoidance manoeuvres etc. This indicates that rolling of a ship moving along a curvilinear trajectory deserves special study and, probably, such a statement should be considered as standard in the future.

Unfortunately, so far, too few studies, if any, related to this situation are known. This is caused not only by a possible underestimation of the problem but also by the lack of suitable mathematical models. Most of such models (Ottosson & Bystrom, 1991, Bailey & Price, 1997, Ayaz & Vassalos, 2003) were models devised primarily for studying manoeuvring motion in waves and with the roll considered as a secondary effect.

A certain exception happened to be a study by Remez (1985) who studied rolling in the steady turn from the viewpoint of the seakeeping safety. However, his mathematical model was deficient in the sense that no manoeuvring-originated forces participated in the roll equation. As result, Remez came to the then obvious conclusion that the maximum attainable absolute values of the roll angle during the turn were always inferior to those reached in the most unfavourable corresponding straight run which is, however, contradicting the common sense and the practice of the ship operations.

Moreover, even in still-water manoeuvring, some ships show quite significant instantaneous heel angle absolute values: over 25deg according to Trägårdh (2003). No doubt, this value can be tangibly amplified when the incident wave's action is added. In addition, it was found that such a large dynamic heel correlated with the dynamic trim. This indicates that the usual 4DOF manoeuvring model is not always able to predict this phenomenon correctly.

On the other hand, a number of 6DOF time-domain seakeeping models appeared (Pawlowski & Bass, 1991, Belenky et al., 2003) which contain certain manoeuvrability elements, such as the rudder and propeller forces and are often complemented with a numerical representation of a simple automatic controller to maintain the straight course, i.e. the canonical seakeeping regime, in the presence of wave disturbances. However, typically such codes miss appropriate description of the hull manoeuvring forces and do not fairly reproduce the ship's behaviour in manoeuvring.

It is rather difficult, anyway, to build a mathematical model equally suitable for manoeuvring and seakeeping studies as the quasi-steady viscous forces are highly essential in the first case while the substantially unsteady potential forces, including the hydrostatic part, dominate in seakeeping. An appropriate direct CFD modelling based on the (still Reynolds-Averaged) Navier–Stokes equations could, in principle, provide adequate description of all physics. But this approach is still highly numerically inefficient even when an exquisite hardware is used. Another problem is connected to difficulties in arranging an appropriate turbulence model which is especially difficult in the highly challenging case of curvilinear motion of a surface displacement ship as the flow around the ship's hull is then rich in separations, re-attachments, vortex formation, let alone substantial interaction with the rudder and propeller. That is why, all practical manoeuvring models are based on empiric data combined with various more or less justified assumptions. As the experimentally determined forces contain also inseparable potential parts, there correct superposition with the seakeeping loads is not trivial.

The present study is based on a newly developed approximate manoeuvring-and-seakeeping mathematical model suitable for slender displacement ships. Some elements of this model are described in (Sutulo & Guedes Soares, 2005). The model is used in this study to model the ship rolling in turning manoeuvres by means of the time-domain simulation of the manoeuvring motion in regular sea of moderate

height and weak steepness. As the used model is nonlinear, and accounts for most coupling effects, it can potentially reveal the parametric resonance, describe the broaching phenomenon in astern sea and the capsizing situations. However, envisaging corresponding studies in the future, this particular contribution does only deal with the situation close to the main roll resonance with the main purpose of comparing the roll's severity in straight runs and in relatively tight manoeuvres. Only full-helm turning manoeuvres are considered here as they can be considered a priori as being of the most dangerous ones, especially at the initial phase which also is similar to the initial phase of many other manoeuvres, like fast course changes, fast lane changes etc.

2. SHIP MATHEMATICAL MODEL

2.1. Frames of Reference

The following right-hand Cartesian frames of reference are used:

The Earth-fixed frame $O_0\xi_0\eta_0\zeta_0$ with the origin O_0 and the ξ_0-axis lying on the undisturbed free surface (some appropriate direction of this axis can be chosen arbitrarily). The ζ_0-axis is directed vertically downwards.

The body axes $Cxyz$ linked to the ship treated as a rigid body. The x-axis lies in the centre-plane of the ship and is directed to the bow. It is supposed that at some initial time moment $t = 0$ and at the ship's equilibrium position this frame coincides with the Earth frame i.e. the z-axis is directed from top to bottom and the y-axis—to the starboard. The body frame's position and orientation with respect to the Earth frame is described by the origin's advance ξ_C, transfer η_C, sinkage (or heave) ζ_C, and by the three Euler angles defined as usual: the heading angle ψ, pitch angle θ and roll angle φ.

The body semi-fixed axes $O\xi\eta\zeta$ differing from the body-fixed axes $Cxyz$ by not being involved into the heave, pitch and roll.

During the evaluation, one more system of co-ordinates $O_1\xi_1\eta_1\zeta_1$ was used which differed from the frame $O\xi\eta\zeta$ by its non-involvement into the wave-induced yawing. These axes are usually called the seakeeping axes in the orthodox linear consideration.

2.2. Basic Equations of Motion

The ship is assumed to be rigid. The Euler equations of motion in the non-central body axes are written as:

$$
\begin{aligned}
&(m+\mu_{11})\dot{u} + (mz_G + \mu_{15})\dot{q} - mvr \\
&-mx_G r^2 + mz_G pr + mwq - mx_G q^2 = X, \\
&(m+\mu_{22})\dot{v} - (mz_G + \mu_{24})\dot{p} + (mx_G + \mu_{26})\dot{r} \\
&+mur - mur - mwp + mx_G pq + mz_G qr = Y, \\
&(m+\mu_{33})\dot{w} - (mx_G + \mu_{35})\dot{q} - muq \\
&-mz_G q^2 + mvp + mx_G pr - mz_G p^2 = Z, \\
&-(mz_G + \mu_{24})\dot{v} + (I_{xx} + \mu_{44})\dot{p} - (I_{xz} + \mu_{46})\dot{r} \\
&+mz_G wp + (I_{zz} - I_{yy})qr - mz_G ur - I_{xz} pq = K, \\
&(mz_G + \mu_{15})\dot{u} - (mx_G + \mu_{35})\dot{w} + (I_{yy} + \mu_{55})\dot{q} \\
&+mx_G uq + mz_G wq + (I_{xx} - I_{zz})pr \\
&+I_{xz}(p^2 - r^2) - mz_G vr - mx_G vp = M, \\
&(mx_G + \mu_{26})\dot{v} - (I_{xz} + \mu_{46})\dot{p} + (I_{zz} + \mu_{66})\dot{r} \\
&+mx_G ur - mx_G wp + (I_{yy} - I_{xx})pq + I_{xz} qr = N,
\end{aligned}
\tag{1}
$$

where m is the ship's mass, x_G and z_G are the centre-of-mass' co-ordinates; X, Y, Z, K, M, N are the total forces and moments for the surge, sway, heave, roll, pitch, and yaw respectively, and u, v, w, p, q, r are the (quasi)-velocities of surge, sway, heave, roll, pitch and yaw respectively.

The dynamic equations are also complemented with the standard kinematic

differential equations linking the generalized ship co-ordinates with the quasi-velocities.

For each force or moment component $F = X, Y, \ldots, N$, the following decomposition takes place:

$$F = F_g + F_{sk} + F_m - F_{sk0}, \tag{2}$$

where the subscripts have the following meaning: g stands for the gravitational forces; sk —seakeeping forces; m —manoeuvring forces; $sk0$ corresponds to the seakeeping forces which are computed at the zero wave amplitude and are subtracted to eliminate double account of potential components present in both the seakeeping and manoeuvring loads. In the slender-body theory, the last component is defined by the zero-frequency added mass longitudinal distribution. When integrated along the reduced ship length to account for viscous effects, as done in the present study, this distribution results in the horizontal plane in the slender-body estimate of the manoeuvring forces which are introduced here independently.

2.3. Seakeeping Forces

Assumptions. The ship is assumed to be slender so that the strip method is applicable and the oncoming waves are regular, with constant parameters. The flow is supposed to be potential and described with the absolute fluid velocity potential $\phi(\xi_0, \eta_0, \zeta_0)$ satisfying the Laplace equation within the fluid domain and all the usual boundary conditions. The free-surface boundary condition is supposed to be linear and satisfied on the undisturbed free surface.

Representation of the Velocity Potential. As usual, the velocity potential can be decomposed as follows:

$$\phi = \phi_r + \phi_w + \phi_d, \tag{3}$$

where ϕ_r is the potential caused by the ship motions, ϕ_w is the incident wave potential, and ϕ_d is the diffraction potential.

The potential ϕ_r satisfies the usual body boundary condition on the instantaneous submerged hull surface S_B and the incident wave potential is taken as

$$\phi_w = \mathrm{Re}\left[\frac{iga_w}{\omega} e^{-k\zeta_0 - i(k_1\xi_0 + k_2\eta_0)} e^{i\omega t}\right], \tag{4}$$

where $k_1 = k\cos\chi_{w0}$, $k_2 = k\sin\chi_{w0}$, $k = \omega^2/g$ is the wave number, ω is the wave frequency, and χ_{w0} is the wave propagation angle with respect to the axis $O_0\xi_0$.

Decomposition of Seakeeping Forces. the ship velocity $\mathbf{V}_C$ is supposed to be constituted of two parts: the steady velocity of advance $\mathbf{V}_{C\mathbf{0}}$ and the seakeeping part per se $\mathbf{V}_{C\mathbf{1}}$. A similar decomposition can be made in a more general seakeeping-and-manoeuvring formulation. For the total velocity of any point fixed in the moving frame $\mathbf{V}(x, y, z)$ it can be written:

$$\mathbf{V}(x, y, z, t) = \mathbf{V}_0(x, y, z, t) + \mathbf{V}_1(x, y, z, t), \tag{5}$$

where the subscript 0 corresponds to the base manoeuvring motion which is assumed to be time-dependent but changing slowly: time derivatives of any variables related to that motion are neglected. The variables with the subscript 1 correspond to the wave-induced motion and their derivatives are not neglectable. The velocity potential can be represented similarly i.e. $\phi = \phi_0 + \phi_1$, where ϕ_0 is the slowly-varying potential associated with the base manoeuvring motion and ϕ_1 is the potential originating from the incident waves' action.

Using the usual Bernoulli pressure equation written in the semi-fixed axes $O\xi\eta\zeta$ and applying the subdivision of the velocity and of the potential into the slow and fast parts the

following representation of the pressure is obtained:

$$p = p_{hs} + p_0 + p_{01} + p_1 + p_2, \qquad (6)$$

where $p_{hs} = \rho g \zeta$ is the hydrostatic pressure; $p_0 = \rho \mathbf{V_0} \cdot \nabla \phi_0 - \frac{1}{2} \rho (\nabla \phi_0)^2$ is the usual quasi-steady contribution whose second term is dropped in linear theories; $p_{01} = \rho \mathbf{V_1} \cdot \nabla \phi_0 - \rho \nabla \phi_0 \cdot \nabla \phi_1$ is the quasi-steady-unsteady interaction part; $p_1 = -\rho(\partial \phi_1 / \partial t) + \rho \mathbf{V_0} \cdot \nabla \phi_1$ is the usual first-order seakeeping contribution, and $p_2 = -\frac{1}{2} \rho (\nabla \phi_1)^2 + \rho \mathbf{V_1} \cdot \nabla \phi_1$ is the pressure creating a part of the second-order seakeeping force, while another second-order contribution stems from the variability of the wetted hull surface over which the total pressure is integrated.

As the total hydrodynamic force **F** and moment **M** are linear functionals of the pressure distribution, they can be decomposed similarly to the pressure itself. The contribution of p_0 will not be considered further as it relates to the manoeuvring part of the forces accounted for outside the potential theory. Similarly, dropped is the part associated with the interaction pressure p_{01} as this part is neglected in most seakeeping theories and can only be important for fast vessels. The part related to p_2 can be essential in manoeuvring problems but is currently dropped for simplification purposes as it constitutes just a part of the second-order force.

The scalar product in the second term in the equation for p_1 can represented as

$$\mathbf{V_0} \cdot \nabla \phi_1 = V_{0\xi} \frac{\partial \phi_1}{\partial \xi} + (V_{0\eta} + \xi r_0) \frac{\partial \phi_1}{\partial \eta}, \qquad (7)$$

where $V_{0\xi,\eta}$ are the ship velocities' projections in the semi-fixed axes.

The first term is present in normal seakeeping theories while the second term appears due to the more general character of the base motion. At present, there are reasons to neglect it as its contribution can only be expected to be comparable to that by the first term at large local drift angles which can only happen in the low-speed manoeuvring when the term containing the local derivative $\partial \phi_1 / \partial t$ will dominate anyway. In addition, on a slender ship this contribution will be mainly compensated by the term $-\rho \nabla \phi_0 \cdot \nabla \phi_1$.

As $\phi_1 = \phi_r + \phi_w + \phi_d$, the force can be decomposed similarly and the radiation force is

$$F_r = \rho \int_S \frac{\partial \phi_r}{\partial t} n_F \, \mathrm{d}S - \rho V_{0\xi} \int_S \frac{\partial \phi_r}{\partial \xi} n_F \, \mathrm{d}S, \qquad (8)$$

where n_F is the generalized projection of the normal **n**.

Connection Between the Frequency Domain and the Time Domain. Considered is the Fourier image $\hat{\phi}(\omega)$ of the unsteady radiation potential $\phi(t)$ (all the spatial arguments are dropped). As a radiation force component $X_{ri}(t), i = 1, \ldots, 6$ is represented as

$$X_{ri} = \rho \int_S \left(\frac{\partial}{\partial t} - V_{0\xi} \frac{\partial}{\partial \xi} \right) \phi_r n_i \, \mathrm{d}S, \qquad (9)$$

its Fourier image is

$$\hat{X}_{ri}(\omega) = i\omega\rho \int_S \hat{\phi}_r n_i \, \mathrm{d}S - \rho V_{0\xi} \int_S \frac{\partial \hat{\phi}_r}{\partial \xi} n_i \, \mathrm{d}S, \qquad (10)$$

where the wetted surface S is supposed to be invariant or depending on the time parametrically so that this could be ignored in evaluating the Fourier transform.

Further, the Fourier transform of the radiation potential is expressed through the radiation functions $\hat{\phi}_1, \ldots, \hat{\phi}_6$ and the complex amplitudes of the generalized velocities $\hat{U}_1, \ldots, \hat{U}_6$ as $\hat{\phi}_r = \sum_{i=1}^{6} \hat{\phi}_i \hat{U}_i$, where $\hat{U}_j = i\omega \hat{\xi}_j$, $j = 1, 4, 5, 6$, $\hat{U}_2 = i\omega \hat{\xi}_2 - V_{0\xi} \hat{\xi}_6$, $\hat{U}_3 = i\omega \hat{\xi}_3 + V_{0\xi} \hat{\xi}_5$, and where $\hat{\xi}_j$ are the displacements' complex amplitudes.

Representation of the first-order force on a slender ship. According to the strip method, the radiation forces in the frequency domain are represented as

$$\hat{X}_{r5} = -\int_{L'} \xi \hat{R}_3(\xi)\,\mathrm{d}\xi,$$
$$\hat{X}_{r6} = \int_{L'} \xi \hat{R}_2(\xi)\,\mathrm{d}\xi, \tag{11}$$

where the integration interval L' is the part of the ship's length depending on the force component and subcomponent in concern, and the transverse loading is:

$$\hat{R}_k = -i\omega \sum_{\ell=2}^{4} \hat{\mu}_{k\ell}(\xi)\hat{u}_\ell(\xi) + V_{0\xi} \sum_{\ell=2}^{4} \frac{\partial}{\partial \xi}[\hat{\mu}_{k\ell}(\xi)\hat{u}_\ell(\xi)],\ \ k = 2,3,4. \tag{12}$$

and where the sectional complex added masses are defined as usual through the complex potential distribution and the sectional generalized velocities are:

$$\hat{u}_2(\xi) = \hat{U}_2 + \xi \hat{U}_6 - \frac{V_{0\xi}}{i\omega}\hat{U}_6,$$
$$\hat{u}_3(\xi) = \hat{U}_3 - \xi \hat{U}_5 + \frac{V_{0\xi}}{i\omega}\hat{U}_5, \quad \hat{u}_4(\xi) \equiv \hat{U}_4. \tag{13}$$

Then, the final relations for the radiation forces on a slender hull in the frequency domain will be

$$\hat{X}_{rj}(\omega) = \sum_{k=2}^{6} \hat{A}_{jk}(\omega)\hat{U}_k(\omega), \quad j = 2,3,\ldots,6, \tag{14}$$

where the complex amplitude functions are:

$$\hat{A}_{jk} = -i\omega\hat{\mu}_{jk} + V_{0\xi}\hat{\bar{\mu}}_{jk}, \quad k = 2,3,4;$$
$$\hat{A}_{j5} = -i\omega\hat{\mu}_{j5} + V_{0\xi}\hat{\bar{\mu}}_{j5} - 2V_{0\xi}\hat{\mu}_{j3} + \frac{V_{0\xi}^2}{i\omega}\hat{\bar{\mu}}_{j3}, \tag{15}$$
$$\hat{A}_{j6} = -i\omega\hat{\mu}_{j6} + V_{0\xi}\hat{\bar{\mu}}_{j6} + 2V_{0\xi}\hat{\mu}_{j2} - \frac{V_{0\xi}^2}{i\omega}\hat{\bar{\mu}}_{j2},$$

Here, the ship complex added masses $\hat{\mu}_{jk}(\omega)$ are obtained through appropriate weighted integration of the sectional complex added masses $\hat{\mu}_{r\ell}(\xi,\omega)$ over the entire ship length L while the quantities $\hat{\bar{\mu}}_{jk}(\omega)$ are obtained similarly but integrated are the derivatives $\partial\hat{\mu}_{r\ell}/\partial\xi$ along the reduced length L'.

These forces are transformed into the time domain by using the method of auxiliary state variables described by Sutulo & Guedes Soares (2005). The resulting model is still a set of ordinary differential equations though of a much higher order (over 200 in the present implementation).

Hydrostatic and Froude–Krylov forces. These forces can be easily computed with the only assumption of the absence of the water surface' deformation due to presence of the ship. In the current implementation, also the longitudinal curvature of the hull surface is neglected. As this force must be estimated with account for the actual wetted surface, the latter is found as the intersection of the entire hull positioned with actual instantaneous values of the heave, pitch and roll with the instantaneous water surface which is described as

$$\zeta_w = -a_w e^{i[\omega t + \Phi(t)]} e^{-ik[\xi\cos(\chi_{w0}-\psi)+\eta\sin(\chi_{w0}-\psi)]}, \tag{16}$$

where $\Phi = -k(\xi_{C0}\cos\chi_{w0} + \eta_{C0}\sin\chi_{w0})$ is the total wave phase and the real part is supposed to be taken. The wave profile at any ship section can be easily determined and this defines approximately the wetted surface at any given instant. The hydrostatic and Froude–Krylov forces $X_{hsk} + X_{wk}$ are then computed as follows:

$$X_{hsk} + X_{wk} = -\rho g \int_S \zeta\,\mathrm{d}S - \rho g a_w e^{i[\omega t+\Phi(t)]} \times \int_S e^{-k\zeta - ik[\xi\cos(\chi_{w0}-\psi)+\eta\sin(\chi_{w0}-\psi)]} n_k\,\mathrm{d}S. \tag{17}$$

Diffraction forces. This part of the excitation forces is also evaluated under the assumption that

the wetted surface doesn't participate in the wave-induced motion although in the final formulae this assumption can be lifted. Then, in the frequency domain, the primary diffraction force representation is quite similar to that for the radiation potential.

After using the second Green identity, the boundary condition $\left(\partial\hat{\phi}_d/\partial n\right)=-\left(\partial\hat{\phi}_w/\partial n\right)$ on S for the diffraction potential, and the Tuck transformation (Salvesen et al., 1970), the following formulae for the Fourier images of the diffraction forces on a slender hull:

$$\begin{aligned}
\hat{X}_{dk} &= \int_L f_{dk}^{(1)}(\xi)\,\mathrm{d}\xi + f_{dk}^{(2)}(\xi_m), \quad i=2,3,4;\\
\hat{X}_{d5} &= -\int_L f_{d3}^{(1)}(\xi)\xi\,\mathrm{d}\xi - \int_{L'} f_{d3}^{(2)}(\xi)\xi\,\mathrm{d}\xi\\
&\quad -\xi_m f_{d3}^{(2)}(\xi_m),\\
\hat{X}_{d5} &= \int_L f_{d2}^{(1)}(\xi)\xi\,\mathrm{d}\xi + \int_{L'} f_{d2}^{(2)}(\xi)\xi\,\mathrm{d}\xi\\
&\quad +\xi_m f_{d2}^{(2)}(\xi_m),
\end{aligned} \tag{18}$$

where ξ_m is the last section corresponding to the end of the length L', $f_{dk}^{(1)}=i\omega f_{dk}$, $f_{dk}^{(1)}=V_{0\xi}f_{dk}$, and

$$\begin{aligned}
f_{dk} &= -\rho\omega a_w e^{i\Phi} e^{-ik\xi\cos(\chi_w-\psi)}\\
&\cdot\int_C [n_2\sin(\chi_w-\psi)-in_3]e^{-k\zeta-ik\eta\sin(\chi_w-\psi)}\hat{\phi}_k\,\mathrm{d}C,
\end{aligned} \tag{19}$$

where $\hat{\phi}_k$ are the two-dimensional radiation functions for each contour C. As within the linear theory at slowly varying base motion parameters, the diffraction force will vary in time almost harmonically i.e. with some slowly varying encounter frequency ω_e, the time domain representation of the diffraction forces will be

$$X_{dk}(t)=\hat{X}_{dk}e^{i\omega_e t} \tag{20}$$

The instantaneous encounter frequency is then estimated as

$$\omega_e=\omega-k(V_{0\xi}\cos\chi_w+V_{0\eta}\sin\chi_w). \tag{21}$$

2.4 Still-Water Manoeuvring Forces

Any suitable still-water manoeuvring mathematical model could be used as the base model for describing the "manoeuvring" contribution F_m. In this particular study, the well-known 4DOF model developed by Inoue et al. (1981) was preferred but the implementation of this model in the wave manoeuvring code had certain peculiarities.

Although the original model is 4DOF, all the hydrodynamic forces depend also on the ship's draught and trim. These two parameters can be assumed to be varying in course of the simulation and this transforms the model into an effectively 6DOF one.

Although the experiment-based yawing moment is dependent on the roll angle, this dependence is only valid for the roll angles not exceeding (or slightly exceeding) 10deg in absolute value. As extension of this range requires additional captive-model tests, in this implementation the regressions were simply extrapolated as constant limiting values.

The angle of attack of the rudder is computed with account for the wave-induced velocities.

3 NUMERICAL RESULTS

3.1 Ship Description

One of the well-known benchmark ships, namely the container ship S-175 was chosen for simulations. The ship's length between the perpendiculars is 175m, breadth 25.4m, draught 9.5m, mass (as estimated) 24571.25 tonnes. The centre of mass' elevation $KG=9.52\text{m}$, the estimated transverse metacentric height $GM=1.02\text{m}$, and the natural roll period is 18s. The body plan of the ship as described in the program's input is shown on Figure 1, with all the input vertices present. More details about the

vessel's particulars can be found in (ITTC, 1983).

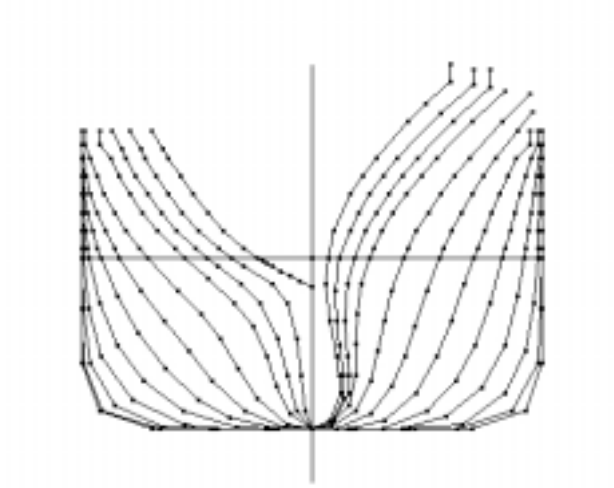

Figure 1 Ship body plan

The ship is directionally stable in still water though the stability margin is rather low. All the simulations were carried out with the approach speed of 15 knots although the design speed for this ship is equal to 22kn. The roll damping coefficient was assumed as recommended by (ITTC, 1983). The simulated decay curve is shown on Figure 2.

3.2 Results of Simulation

Sea Conditions. All simulations, except those in still water, were performed on regular beam seas (at least, at the approach phase) with the steepness 1/80 and with three frequencies:

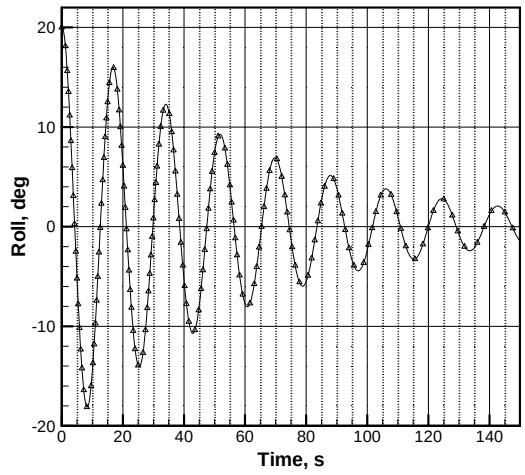

Figure 2 Roll decay curve

$0.35s^{-1}$ corresponding to the ship's natural frequency in roll, $0.292s^{-1}$ and $0.403s^{-1}$.

Constrained Straight Runs. Strictly straight runs were simulated to validate the code against the results available for this ship. Instead of using an autopilot, the ship was artificially constrained in heading and in the rate of yaw. Additional constraints were also tried for all the degrees of freedom except for the roll and surge but that did not change the roll output substantially. Truncated time histories for the three mentioned wave frequencies are presented on Figures 3 through 5. Further simulations did not reveal changes in the ship's behaviour. A good or reasonable agreement with the published amplitude data was found for roll (demonstrated below) as well as for other motions.

Free Straight Runs. Free runs with the rudder fixed in neutral position were simulated as well. In still water such simulation do not lead to interesting results as the ship keeps on the straight path for long, and are mainly used for checking purposes.

The situation changes dramatically in a seaway as an uncontrolled ship in still water and in absence of wind is never directionally asymptotically stable and can change her heading. In most cases, these changes are performed at a relatively low rate (except for the case of broaching not considered here) but under continuous action of the wave excitation forces the resulting trajectory becomes substantially curvilinear and periodic with the lowest harmonic's frequency much inferior to the instantaneous wave encounter frequency.

The time histories for the resonance case and the simulation time 50 minutes are presented on Figures 6 and a stretched 200s interval of the same process—on Figure 7. It is clearly seen that the wave-induced oscillations are modulated with a much lower frequency corresponding to the ship's spontaneous course performing a sequence of turns and a similar picture was observed with

the waves below and above resonance. However, all these cases correspond to significant although low-slope regular waves with the height varying from 4.7 to 9 meters and such behaviour doesn't seem impossible for a beam sea directed initially to the starboard.

Several simulations on lower-height waves resulted in trajectories without intersections i.e. the ship was meandering. However, in all the cases of spiralling or meandering, the ship in the mean was displacing strait, along some oblique virtual path.

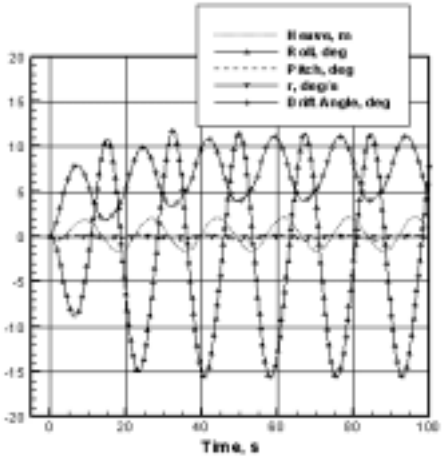

Figure 3 Constrained straight run time histories at the resonance wave frequency $\omega = 0.35$

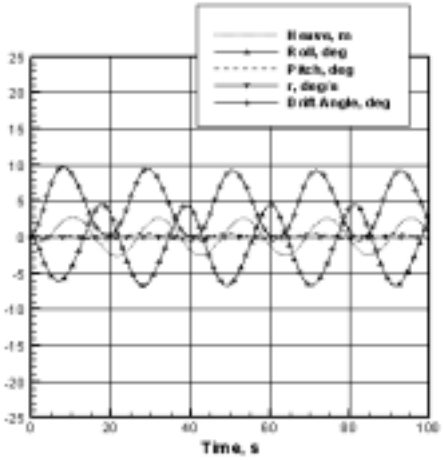

Figure 4 Constrained straight run time histories at $\omega = 0.292$

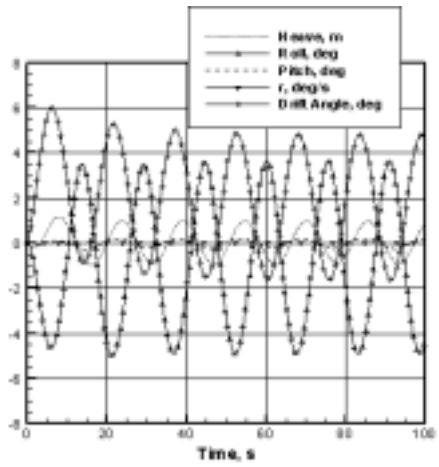

Figure 5 Constrained straight run time histories at $\omega = 0.403$

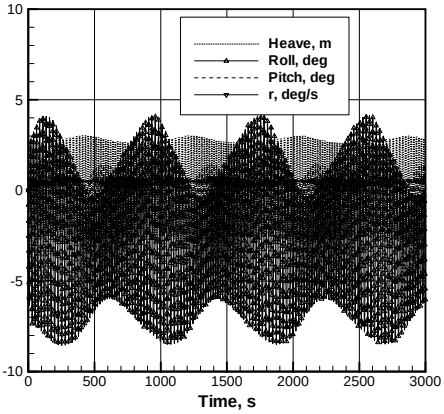

Figure 6 Free straight run time histories at $\omega = 0.35$

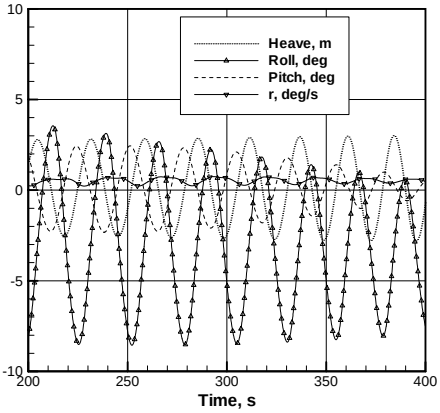

Figure 7 Free straight run: time histories at $\omega = 0.35$ (stretched)

In other words, the ship becomes in a certain sense directionally asymptotically stable in the

average while this can never happen in still water and in absence of wind. A somewhat similar result was obtained by Ananyev & Gorbachova (1993) through analysis of stability of the motion described by a linear equation of yaw with periodically varying coefficients. However, as the mathematical models are very different, it still cannot be stated with certainty that in the both cases the same phenomenon was traced.

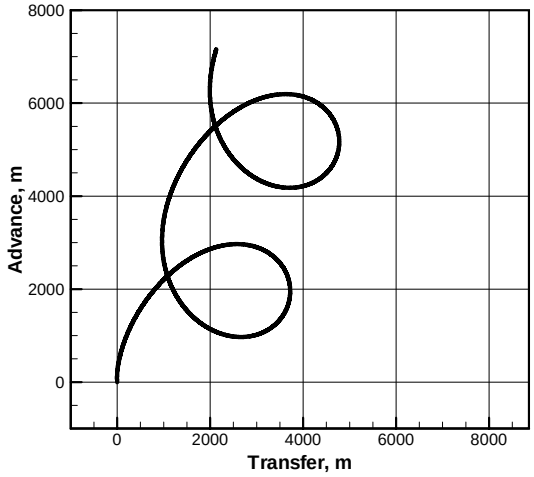

Figure 8 Free straight run trajectory at $\omega = 0.35$

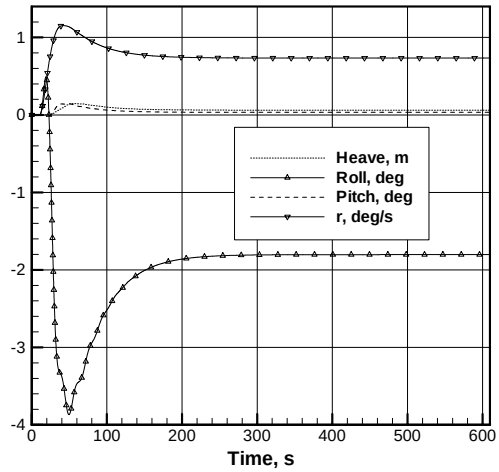

Figure 9 Turning manoeuvre: time histories in still water

Turning Manoeuvres. First, the turn with the 35 degrees helm was simulated in still water to reveal the roll triggered by the manoeuvre per se. Time histories for several kinematic parameters are shown on Figure 9. As usual, after a small yank inwards, the ship rolls outside the turn reaching dynamically 4 degrees in this case but the steady turn for this relatively stable ship and low approach speed is less than two degrees.

Then, simulations of the same turn but on the roll-resonant regular waves were performed with different values of the manoeuvre delay time which is the time interval between the beginning of simulation and the start of the rudder's deflection. The minimum delay time was assumed to be 24s as judging from the straight run simulations, the rolling is practically developed by this time. Then the delay was varied with the 4.5s increment which was one quarter of the roll period.

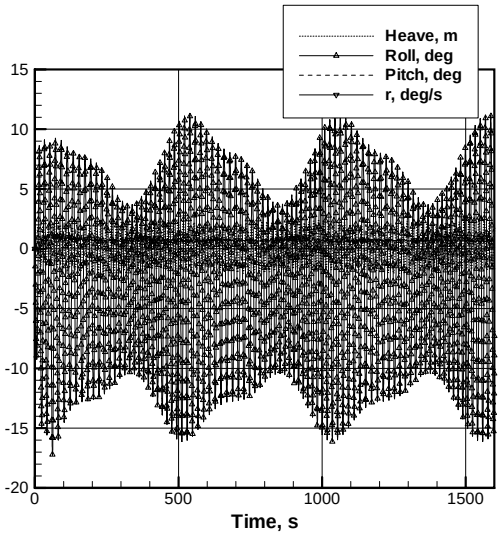

Figure 10 Turning manoeuvre: time histories at $\omega = 0.35$

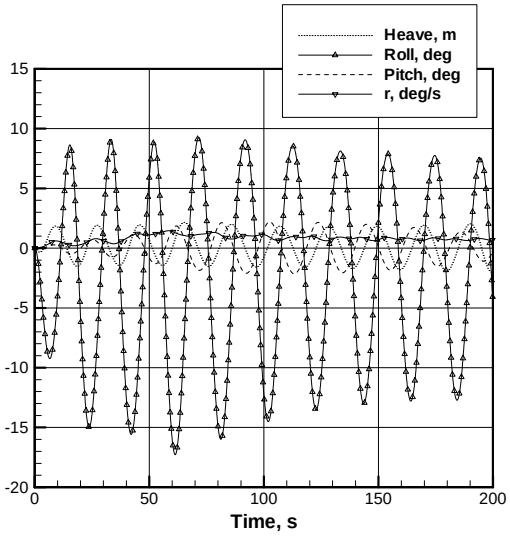

Figure 11 Turning manoeuvre: time histories at $\omega = 0.35$ (stretched).

As the largest observed absolute values of the instantaneous roll angle corresponded to the 33s delay, all the displayed results refer to this case.

The full time histories are shown on Figure 10 and their stretched cut-off—on Figure 11. Qualitatively, the general view of the time histories did not differ too much from the free straight runs case but the period is different and they show more asymmetry with respect to the zero-roll line. This is explained by tighter turns with the rudder's assistance (Figure 12).

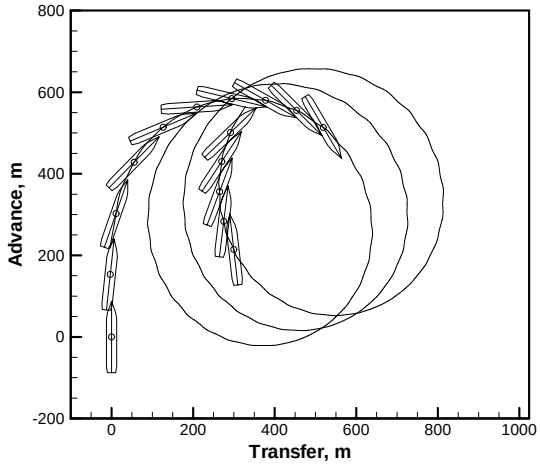

Figure 12 Turning manoeuvre: trajectory at $\omega = 0.35$; ship images are only shown for the initial and final phases of the simulation

3.3 Discussion of Results

As one of the main objectives of the present study was to check whether manoeuvring in waves is indeed a more dangerous regime than the straight run in beam seas, various numerical measures of the roll were extracted from the simulation outputs. These values are given in Table 1 together with the values of the roll amplitude obtained by different towing tanks and published by ITTC (1983).

The values of the amplitudes obtained with the present code in the constrained-run simulations agree well with the values obtained by other programs in the same conditions and this indicates credibility of further results referring to less typical situations.

It is seen from the table data that both the amplitudes and the maximum values are smaller in free straight runs than in the constrained runs representing the canonical seakeeping situation. This is likely due to a relatively short period of time when the ship is exposed to the least favourable conditions: the beam sea and the resonance (or close to resonance) effective encounter frequency. However, in 35deg turns the situation was different: the maximum reached roll angles and even amplitudes were higher than in the strictly straight run. This result, however, was not unexpected and is explained by the combined action of the seakeeping and manoeuvring moments.

Table 1: Numerical Measures of Roll

Measure	Conditions	Wave frequency, rad/s		
		0.292	0.35	0.403
(Maximum) Roll Amplitude	constrained straight run	5.75	12.5	5.0
	free straight run		6.5	
	ITTC data	4.5–6.3	10.8–14.6	3.4–6.1
	35deg helm turn		14.1	
Maximum Reached Values of Roll Angle	constrained straight run	6.0	15.5	4.4
	free straight run		8.5	
	35deg helm turn		17.2	

These results are considered as primary and still no search was made for the situation when the synergetic effect will be more pronounced. For instance, increase of the approach speed and reduction of the metacentric height will by all means lead to a much stronger effect of the tuning motion in rolling assessments. Using a turning manoeuvre instead of the straight run could have another advantage: this manoeuvre can be effectively executed without any artificial constraints, on the one hand but also without any automatic controller in the loop whose parameters can influence the resulting estimates.

4. CONCLUSIONS

Primary simulations of the roll motion of a displacement ship have been carried out with a manoeuvring-and-seakeeping code newly developed by the authors. Although these results are primary and the chosen simulation conditions were not the most characteristics in all the respects, certain conclusions can already be drawn. These are:

The roll motion in a turning manoeuvre in regular waves is modulated by some low frequency corresponding to the completion of the ship's full turn.

Qualitatively, the same behaviour is observed in the so-called free straight runs in waves i.e. when the rudder is fixed in the neutral position: the ship is in fact turning with some low rate approximately in the direction of the propagation of the waves.

The roll amplitudes did not differ much for all the three studied manoeuvres (constrained straight run, free straight run, turning manoeuvre).

Due to some roll asymmetry caused partly by the nonlinearity of the used model, and partly by the manoeuvring-originated forces, the attained absolute values of the roll angle are greater then the amplitude values.

The largest instantaneous absolute values of the roll were observed in the initial phase of the turning manoeuvre due to a synergy of the wave action and of roll moment due to manoeuvring.

Tight turns have certain advantages over the straight free runs as reference motion for the roll analysis with time-domain mathematical models.

5. ACKNOWLEDMENTS

The first author was partly financed by The Portuguese Science and Technology Foundation (Fundação da Ciência e Tecnologia), under the grant SFRH/BPD/8557/2002.

6. REFERENCES

Ananyev, D.M. and Gorbachova, L.M., 1993, "Applied Problems of Ship Manoeuvring in Waves", Technical University for Fishing Publ., Kaliningrad, 151p. (in Russian).

Ayaz, Z. and Vassalos, D., 2003, "Towards an Improved Mathematical Model for Ship Manoeuvring in Astern Seas", Proceedings. of MARSIM'03, Kanazawa, Japan, August 25-28, pp. RC-14-1–RC-14-10.

Belenky, V.L., Weems, K.,M., Liut, D., Shin, Y.S., 2003, "Nonlinear Roll with Water-on-Deck: Numerical Approach", Proc. of STAB'03: 8th International Conference on Stability of Ships and Ocean Vehicles, Madrid, Spain, pp. 59-79.

Bailey, P.A., Price, W.G., Temarel, P., 1997, "A Unified Mathematical Model Describing the Manoeuvring of a Ship Travelling in a Seaway", Trans. RINA, pp. 131-149.

ITTC, 1983, "Summary of Results Obtained with Computer Programs to Predict Ship Motions in Six Degree of Freedom and Related Responses", Report on 15th and 16th ITTC Seakeeping Committee Comparative Study on Ship Motion Program (1976-1981), 53p.

Ottosson P. and Bystrom L., 1991, "Simulation of the Dynamics of a Ship Manoeuvring in Waves", SNAME Transactions, Vol. 99, pp. 281-298.

Pawlowski, J. and Bass, D.W., 1991, "A Theoretical and Numerical Model of Ship Motions in Heavy Seas", SNAME Transactions, Vol. 99, pp. 319-352.

Remez, V., 1985, "Dynamics of Curvilinear Motion of a Ship in Regular Seas", 5th National Congress on Theoretical and

Applied Mechanics and 14th Scientific and Methodological Seminar on Ship Hydrodynamics, Varna, Bulgaria, 23-29 September 1985, Proceedings, Vol. 1, pp. 2-1-2-7.

Salvesen, N., Tuck, E.O., Faltinsen, O.M., 1970, “Ship Motions and Sea Loads”, SNAME Transactions, Vol. 78, pp. 250-287.

Sutulo, S., Guedes Soares, 2005, C. “An Implementation of the Method of Auxiliary State Variables for Solving Seakeeping Problems”, International Shipbuilding Progress, Vol. 52, No. 4, pp. 363-390.

Trägårdh, P., 2003, “Roll Motion of Manoeuvring Ships”, Proceedings. of MARSIM’03, Kanazawa, Japan, August 25-28, pp. RC-9-1–RC-9-5.